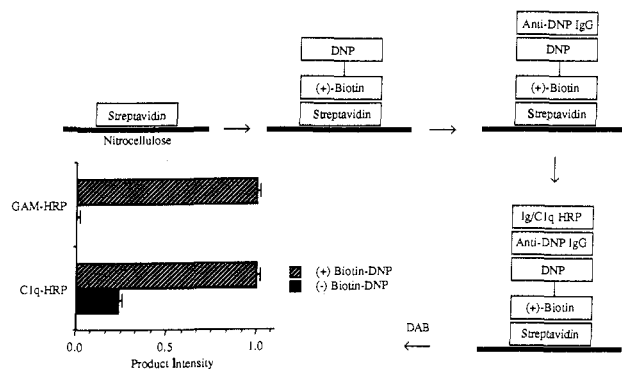


Figure 1. Schematic diagram of ligand-mediated immunogenicity.

Scheme II



tetrahydrochloride (DAB) and H_2O_2 (HRP substrates) at 4 °C and quantitated by densitometry of a positive exposure of the filter (Scheme I).¹⁹ A control lacking CD4-DNP was performed to test for nonspecific binding of the anti-DNP antibody and the GAM-Ig-HRP conjugate. Controls lacking gp120 but containing CD4-DNP showed no signal (data not shown). In contrast, a large signal was obtained for the ELISA containing gp120, CD4-DNP, anti-DNP antibody, and GAM-Ig-HRP, indicating the successful targeting of antibodies to gp120 via noncovalently introduced epitopes.

The ability of the CD4-DNP gp120 complex to activate complement was assayed by substitution of C1q-HRP for GAM-Ig-HRP in the experiment described above. The first component of complement, C1q, is responsible for triggering the complement cascade to destroy cells on which immune complexes form.¹⁷ C1q-HRP bound specifically relative to a control lacking CD4-DNP (Scheme I), demonstrating the successful formation of an immune complex on gp120, mediated by a noncovalently introduced epitope.²⁰

In order to demonstrate the ability of small molecules to direct anti-DNP antibodies to proteins, a biotin-DNP linker was synthesized. Biotin-DNP was synthesized by condensation of DNP-tetraethylene glycol diamine and biotin using dicyclohexylcarbodiimide. Streptavidin was bound to nitrocellulose, and the sandwich assay was performed as described above (Scheme

(19) To a 3-mm-diameter circle of nitrocellulose was added 50 μ L of gp120 (100 μ g/mL) (30 min), and excess protein binding sites were blocked with a 3% BSA solution (2 h), followed by addition of CD4-DNP. (+) CD4-DNP = 100 μ L (25 μ g/mL) of CD4-DNP (30 min); (-) CD4-DNP = no CD4-DNP added. One hundred microliters (8 μ g/mL) of anti-DNP antibody AN09 (30 min) was added followed by either 100 μ L (1 μ g/mL) of GAM-Ig-HRP (30 min) or 100 μ L (10 μ g/mL) of C1q-HRP (30 min). DAB substrate (4 °C) was added to the washed nitrocellulose. Product intensity was determined by a laser densitometer scan of a film positive of the nitrocellulose.

(20) The decrease in the ratio of specific to nonspecific binding of C1q-HRP compared to GAM-Ig-HRP is due to the low affinity of C1q for monomeric mouse IgG2a. C1q is hexameric and thus binds to aggregated IgG with great avidity ($K_A = 10^8 M^{-1}$)²² but binds monomeric IgG poorly ($K_A = 10^4 M^{-1}$).²³ Because nitrocellulose is a solid support, the anti-DNP antibodies remain fixed rather than being able to aggregate or "cap" as they would on the surface of a cell. Goat anti-mouse-Ig antibodies typically have relatively high affinities ($K_A = 10^7$ - $10^9 M^{-1}$) for monomeric IgG and thus give a much better signal-to-noise ratio in this type of assay.

II).²¹ Again the biotin-DNP conjugate successfully targeted anti-DNP antibody to streptavidin. A functional assay substituting C1q-HRP for GAM-Ig-HRP shows that the protein sandwich can also trigger a complement response. Streptavidin contains four biotin binding sites and thus may provide a better mimic of "capping" of antibodies on the surface of cells. Anti-DNP antibody also binds specifically to immobilized streptavidin in the presence of an excess of free biotin-DNP relative to the control lacking biotin-DNP.

Acknowledgment. We thank Brenda Baker and Dan Littman for the generous supply of sCD4 and helpful discussions and Harden McConnell for supplying hybridoma cell line AN09. We also thank Carolyn Bertozzi for helpful discussions. This work was supported by the Director, Office of Energy Research, Office of General Life Sciences, Structural Biology Division, of the U.S. Department of Energy under Contract No. DE-AC0376SF00098. P.G.S. is a W. M. Keck Foundation Investigator.

Supplementary Material Available: Full spectroscopic and analytical data for all compounds and experimental details (4 pages). Ordering information is given on any current masthead page.

(21) Streptavidin (50 μ L of 100 μ g/mL) was substituted for gp120. Biotin-DNP (100 μ L of 10 μ g/mL) was substituted for CD4-DNP. GAM-Ig-HRP concentration was 2 μ g/mL.

(22) Emanuel, E. J.; Brampton, A. D.; Burton, D. R.; Dwek, R. A. *Biochem. J.* **1982**, *205*, 361-372.

(23) Sledge, C. R.; Bing, D. H. *J. Mol. Biol.* **1981**, *148*, 191-197.

Exploration of New Cooperative Proton-Electron Transfer (PET) Systems. First Example of Extended Conjugated Quinhydrone: 1,5-Dihalo-2,6-naphthoquinhydrone

Kazuhiro Nakasuji,^{*,1a} Kenichi Sugiura,^{1a}
Toshikazu Kitagawa,^{1a} Jiro Toyoda,^{1a} Hiroshi Okamoto,^{1a}
Kaoru Okaniwa,^{1a} Tadaaki Mitani,^{1a} Hiroshi Yamamoto,^{1b}
Ichiro Murata,^{1b} Atsushi Kawamoto,^{1c} and Jiro Tanaka^{1c}

Institute for Molecular Science
Myodaiji, Okazaki 444, Japan
Department of Chemistry, Faculty of Science
Osaka University, Toyonaka, Osaka 560, Japan
Department of Chemistry, Faculty of Science
Nagoya University, Chikusa-ku, Nagoya 464, Japan

Received November 6, 1990

Quinones² have been utilized to produce novel charge-transfer (CT) complexes near the neutral-ionic interface.^{3,4} Renewed

(1) (a) Institute for Molecular Science. (b) Osaka University. (c) Nagoya University.

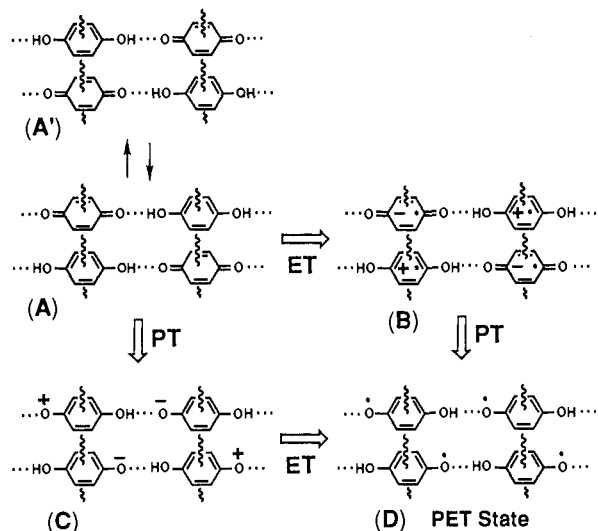


Figure 1. Schematic representation of proton-electron transfer (PET) phenomena in quinhydrone.

attention to the ability of quinones to form a CT state accompanied by hydrogen bonding (H-bonding) has led to finding a new phase transition for 1,4-benzoquinhydrone (BQH) under hydrostatic pressure.⁵ From the phase transition, which can be assigned to cooperative proton-electron transfer (PET) phenomena, we can develop a new concept and a general strategy to explore new materials based on quinhydrone characterized as H-bonded CT complexes. We now propose such a strategy and report the synthesis and some solid-state properties for the first examples of extended conjugated quinhydrone, 1,5-dihalo-2,6-naphthoquinhydrone, which also showed a similar phase transition under pressure.

PET reactions in H-bonded systems have been a prolonged subject of experimental and theoretical interest.⁶ Recently, investigation of such reactions has been expanded to the solid state through progress in experimental techniques. For example, quinhydrone has been shown to undergo an *intermolecular* PET reaction, a redox rearrangement, as schematically shown in Figure 1 (A = A').⁷ As for *intramolecular* PET reactions,⁸ there are

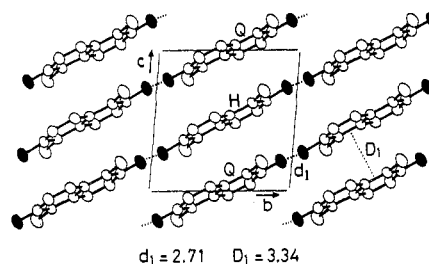


Figure 2. View of the two-dimensional hydrogen-bonded CT networks in CNQH.

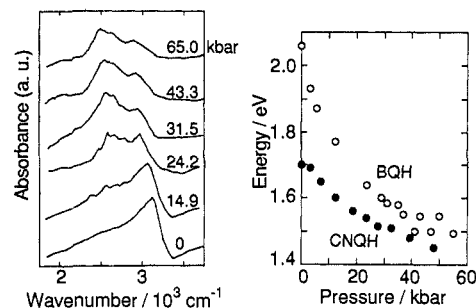


Figure 3. Pressure dependence (left) of the absorption spectra in the O-H stretching regions for CNQH and (right) of the CT transition energies for BQH and CNQH.

intensive investigations on the tautomerism ($\text{NH}\cdots\text{N}=\text{N}\cdots\text{HN}$), for example, in azophenine⁶ and dibenzotetraaza[14]annulene.⁹ General features of these phenomena in the solid state are *multiple* (in these cases, double) modes of PET reactions between closed-shell structures in the initial and the final states. Details of the possible intermediate states with open-shell structures, the PET states, have begun to unravel.⁶

Our particular attention is concentrated on stabilization of such a PET state by using the combined chemical interactions between H-bonding and CT present in the solid. The prototype is the phase transition found for BQH under pressure induced by physical means.⁵ Considering the reaction as if it were stepwise, we can visualize the phase transition on a molecular level as shown in Figure 1. Thus, the PET state might be produced by single ET associated with single PT (A \rightarrow B \rightarrow D), or single PT associated with single ET (A \rightarrow C \rightarrow D). The search for the realization of such a cooperative PET state under milder physical conditions, ambient conditions in particular, can open a new approach to potentially interesting solid-state properties. Neglecting the quantum-mechanical mixing, or CT interaction between the A and B (or C and D) states and proton tunneling between the A and C (or B and D) states, the final PET state (D) can be characterized as a molecular assembly of *H-bonded neutral radicals*.

From the stepwise consideration, two reasonable molecular design strategies for realization of such cooperative PET systems in the solid state are revealed: (a) the exploration of a quinone-hydroquinone pair with a smaller intermolecular CT gap to stabilize the PET state through the excess charge effect on PT¹⁰ and (b) the direct stabilization of the PET state by introducing donor and acceptor groups into quinhydrone.¹¹ Preliminary investigations along the latter (approach b) are now in progress.¹²

The former approach (a) can be pursued through extended conjugated quinhydrone. We prepared 1,5-dichloro-, and 1,5-dibromo-2,6-naphthoquinones (**1a**¹³ and **2a**¹⁴),¹⁵ 1,6- and 1,8-

(2) (a) Bernstein, J.; Cohen, M. D.; Leiserowitz, L. In *The Chemistry of Quinonoid Compounds*; Patai, S., Ed.; John Wiley & Sons Ltd.: Chichester, 1974; pp 37-110. (b) Foster, R.; Foreman, M. I. In *The Chemistry of Quinonoid Compounds*; Patai, S., Ed.; John Wiley & Sons Ltd.: Chichester, 1974; pp 257-333. (c) Depew, M. C.; Wan, J. K. S. In *The Chemistry of Quinonoid Compounds*; Patai, S.; Rappoport, Z., Eds.; John Wiley & Sons Ltd.: Chichester, 1988; Vol. II, pp 963-1018.

(3) Nakasuji, K.; Sasaki, M.; Kotani, T.; Murata, I.; Enoki, T.; Imaeda, K.; Inokuchi, H.; Honda, M.; Kawamoto, A.; Tanaka, J. *J. Am. Chem. Soc.* **1987**, *109*, 6970-6975. Torrance, J. B.; Mayerle, J. J.; Lee, V. Y.; Bechgaard, K. *Ibid.* **1979**, *101*, 4747-4748.

(4) Torrance, J. B.; Vazquez, J. E.; Mayerle, J. J.; Lee, V. Y. *Phys. Rev. Lett.* **1981**, *46*, 253-257. Torrance, J. B.; Girlando, A.; Mayerle, J. J.; Crowley, J. I.; Lee, V. Y.; Batail, P.; LaPlaca, S. *J. Phys. Rev. Lett.* **1981**, *47*, 1747-1750.

(5) Mitani, T.; Saito, G.; Urayama, H. *Phys. Rev. Lett.* **1988**, *60*, 2299-2302. Mitani, T. *Mol. Cryst. Liq. Cryst.* **1989**, *171*, 343-355. Mitani, T. *Synth. Met.* **1988**, *27*, B499-B508.

(6) Rumpel, H.; Limbach, H. *J. Am. Chem. Soc.* **1989**, *111*, 5429-5441. This article quotes leading entries to extensive literatures for *intra-* and *intermolecular* multiple proton transfer reactions not only in the liquid but also in the solid state.

(7) Brodskii, I.; Gragerov, I. P. *Dokl. Akad. Nauk SSSR* **1951**, *79*, 277-279. Kalninsk, K. K. *J. Chem. Soc., Faraday Trans. 2* **1982**, *78*, 327-337. Patil, A. O.; Curtin, D. Y.; Paul, I. C. *J. Am. Chem. Soc.* **1984**, *106*, 4010-4015. Scheffer, J. R.; Wong, Y.-F.; Patil, A. O.; Curtin, D. Y.; Paul, I. C. *Ibid.* **1985**, *107*, 4898-4904. Patil, A. O.; Pennington, W. T.; Desiraju, G. R.; Curtin, D. Y.; Paul, I. C. *Mol. Cryst. Liq. Cryst.* **1986**, *134*, 279-304.

(8) As for the tautomerism ($\text{C}=\text{O}\cdots\text{HO}-\text{C}=\text{C}-\text{OH}\cdots\text{O}=\text{C}$) in naphtharazin and 9-hydroxyphenalenone in solution and/or in the solid state, see, for example: de la Vega, J. R. *Acc. Chem. Res.* **1982**, *15*, 185-191. Haddon, R. C. *J. Am. Chem. Soc.* **1980**, *102*, 1807-1811. Rossetti, R.; Rayford, R.; Haddon, R. C.; Brus, L. E. *Ibid.* **1981**, *103*, 4303-4307. Bondybej, V. E.; Haddon, R. C.; Rentzepis, P. M. *Ibid.* **1984**, *106*, 5969-5973. Kunze, K. L.; de la Vega, J. R. *Ibid.* **1984**, *106*, 6528-6533.

(9) Wehrle, B.; Limbach, H. H.; Zimmermann, H. *J. Am. Chem. Soc.* **1988**, *110*, 7014-7024 and references cited therein.

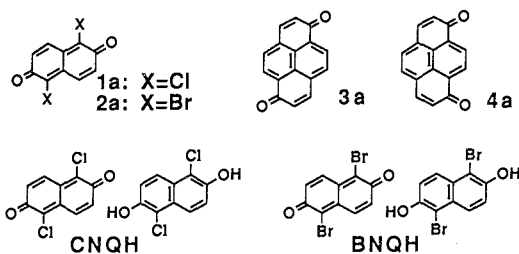
(10) Hasegawa, H.; Daiyasu, K.; Yomosa, S. *J. Phys. Soc. Jpn.* **1970**, *28*, 1304.

(11) Viehe, H. G.; Janousek, Z.; Merenti, R. *Acc. Chem. Res.* **1985**, *18*, 148-154 and references cited therein.

(12) Kitagawa, T.; Toyoda, J.; Nakasuji, K.; Yamamoto, H.; Murata, I. *Chem. Lett.* **1990**, 897-900.

(13) Willstätter, R.; Parnas, J. *Ber. Dtsch. Chem. Ges.* **1907**, *40*, 3971-3978.

pyrenoquinones (**3a** and **4a**),¹⁶ and their corresponding hydroquinones (**1b-4b**).¹⁷ Grinding¹⁸ a solid quinone and hydroquinone



gave powders of the corresponding quinhydrone.¹⁹ The CT transition energies (eV) measured for the compressed pellets of powders dispersed into KBr are 1.70, 1.58, 1.43, and 1.42 eV for **1a-1b**, **2a-2b**, **3a-3b**, and **4a-4b**, respectively. Apparently, smaller energies of the CT gaps are observed for these extended conjugated quinhydrone compared with that of BQH (2.34 eV).

Single crystals of **1a-1b** (CNQH) and **2a-2b** (BNQH) were successfully grown by a diffusion method in benzene as black lustrous plates. Their crystal structure analysis showed the alternately stacked quinone and hydroquinone components and the existence of two-dimensional H-bonded CT networks (Figure 2).²⁰ These are the first examples of the *extended conjugated quinhydrone* whose characteristic features are similar to those of BQH.²⁴ Similarly, the four extended conjugated quinhydrone have shown pressure-response spectral characteristics.²⁵ Thus, Figure 3a presents this type of behavior for the O-H stretching region of CNQH as a typical example. New bands appearing around 2500 cm⁻¹ at higher pressure can be attributed to the contribution of a PET state. In addition, electronic absorption spectra in the CT transition energy regions showed decreasing energies with increasing pressure. Figure 3b presents such a behavior for CNQH, together with that of BQH.

In conclusion, the extended conjugated quinhydrone confirm our molecular design strategy for stabilization of the cooperative

PET systems formed by H-bonded neutral radicals. A closer insight into the concept and design strategy might lead to a new aspect of molecular assemblies with unique solid-state properties originated in the PET radicals.

Acknowledgment. This work was supported in part by a Grant-in-Aid for Scientific Research on Priority Areas (No. 01648003) from the Ministry of Education, Science and Culture, Japan.

Supplementary Material Available: Tables 1-11 of crystal data, final atomic coordinates, equivalent isotropic thermal parameters, intramolecular distances and angles, and final thermal parameters of non-H atoms for the crystal structures of CNQH, BNQH, and **1b** and experimental details of the crystal growth of CNQH and BNQH (10 pages). Ordering information is given on any current masthead page.

Racemization and Geometrical Isomerization of (2*S*,3*S*)-Cyclopropane-1-¹³C-1,2,3-*d*₃ at 407 °C: Kinetically Competitive One-Center and Two-Center Thermal Epimerizations in an Isotopically Substituted Cyclopropane

Steven J. Cianciosi,[†] N. Rangunathan,[†]
Teresa B. Freedman,^{*,†} Laurence A. Nafie,^{*,†}
David K. Lewis,^{*,†} David A. Glenar,^{†,§} and
John E. Baldwin^{*,†}

Departments of Chemistry
Syracuse University, Syracuse, New York 13244
Colgate University, Hamilton, New York 13346

Received November 16, 1990

Shortly after the thermal interconversion of the *cis* and *trans* isomers of 1,2-dideuteriocyclopropane was discovered in 1958,¹ Setser and Rabinovitch² recognized that if one could only determine rate constants k_i and k_{ij} corresponding to one-center and two-center epimerization processes for substituted cyclopropanes, one would have some basis for discriminating among alternative mechanistic models. For a number of substituted cyclopropanes, this desideratum has been achieved,³ but for cyclopropanes substituted only with isotopic labels—systems most relevant to theoretical work on these stereomutations and trimethylene diradical transition structures—it has remained an unmet challenge. We now report that by preparing the chiral isomers of cyclopropane-1-¹³C-1,2,3-*d*₃ and following the thermal stereomutations summarized in scheme I, a determination of the relative importance of these two types of stereomutation processes in the parent hydrocarbon has finally been secured.

These isotopically labeled cyclopropanes are ideally suited for the problem at hand, since each carbon-carbon bond is CHD-CHD and thus, neglecting possible very small ¹³C kinetic isotope effects, only two epimerization rate constants must be found: k_1 and k_{12} . Here k_1 represents the rate constant for one-center epimerization at a single carbon atom when one adjacent C-C bond breaks. There are two experimentally accessible kinetic parameters, $k_1 = (8k_1 + 4k_{12})$, for the rate of approach to equilibration of the geometrical isomers, and $k_a = (4k_1 + 4k_{12})$, for the rate of loss of optical activity.

Syntheses of both chiral forms of the quadruply labeled cyclopropane depended on the reaction of methyl propenoate-3-¹³C-2,3-*d*₂ with methyl chloroacetate-2,2-*d*₂ in DMSO-*d*₆ promoted

(14) **2a** was prepared by a similar procedure to that used for preparation of **1a**.

(15) The reduction potentials (V vs SCE) of the quinones: **1a**, -0.09; **2a**, -0.09, in Et₄NClO₄/dimethylformamide. **3a**, -0.44, -0.79; **4a**, -0.44, -0.80, in *n*-Bu₄NClO₄/benzonitrile.

(16) Fatiadi, A. J. *J. Chromatogr.* **1965**, *20*, 319-324.

(17) **1b**: ref 10. **2b**: Paul, von H.; Zimmer, G. *J. Prakt. Chem.* **1962**, *4*, 219-224. **3b** and **4b**: Tintel, C.; Terheijden, J.; Lugtenburg, J.; Cornelisse, J. *Tetrahedron Lett.* **1987**, *28*, 2057-2060.

(18) Patil, A. O.; Curtin, D. Y.; Paul, I. C. *J. Am. Chem. Soc.* **1984**, *106*, 348-353. Rastogi, R. P.; Singh, N. B. *J. Phys. Chem.* **1966**, *70*, 177-180.

(19) The four new quinhydrone gave satisfactory elemental analyses as having 1:1 stoichiometry.

(20) Crystal data were collected on a Rigaku AFC-5R diffractometer with graphite-monochromated Cu K α radiation. The structures were solved by the Monte Carlo direct method²¹ with the aid of the MULTAN-78 program system²² and refined on F^2 by a full-matrix least-squares technique with analytical absorption correction.²³ Two independent molecules which lie on an inversion center were found in each crystal. H atoms on carbons were allocated from a differential Fourier map and were refined with isotropic temperature factors equivalent to the bonded carbon atoms. H atoms of oxygens were not found. The quinone and the hydroquinone components can unambiguously be distinguished by comparing the bond lengths. Crystal data are as follows: **1a-1b**, C₂₀H₁₀Cl₂O₄, triclinic, $P1$, $Z = 1$, $a = 7.487$ (7) Å, $b = 8.121$ (7) Å, $c = 7.763$ (4) Å, $\alpha = 80.93$ (6)°, $\beta = 102.59$ (7)°, $\gamma = 110.59$ (7)°, $V = 429.4$ (7) Å³, $D_{\text{measd}} = 1.75$, $D_{\text{calcd}} = 1.77$, $R = 0.063$, $R_w = 0.062$; **2a-2b**, C₂₀H₁₀Br₂O₄, triclinic, $P1$, $Z = 1$, $a = 7.703$ (2) Å, $b = 8.041$ (1) Å, $c = 7.926$ (2) Å, $\alpha = 81.12$ (2)°, $\beta = 99.16$ (2)°, $\gamma = 108.61$ (1)°, $V = 455.9$ (2) Å³, $D_{\text{measd}} = 2.37$, $D_{\text{calcd}} = 2.31$, $R = 0.048$, $R_w = 0.053$. The interplanar distances between the donor and the acceptor are 3.32 and 3.36 Å, and the hydrogen-bonded O...O distances are 2.712 (7) and 2.727 (7) Å, for CNQH and BNQH, respectively.

(21) Furusaki, A. *Acta Crystallogr.* **1979**, *A35*, 220-224.

(22) Main, P.; Hull, S. E.; Lessinger, L.; Germain, G.; Declercq, J. P.; Woolfson, M. M. *MULTAN78*; Universities of York and Louvain: York, England, and Louvain, Belgium, 1978.

(23) Katayama, C.; Sakabe, N.; Sakabe, K. *Acta Crystallogr.* **1972**, *A28*, S207.

(24) Sakurai, T. *Acta Crystallogr.* **1965**, *19*, 320-330. Sakurai, T. *Acta Crystallogr.* **1968**, *B24*, 403-412.

(25) The optical characterizations of the PET systems under high pressures will be published elsewhere. The EPR study which gives a more direct proof of the presence of the neutral radical state is under investigation.

[†]Syracuse University.

[‡]Colgate University.

[§]Present address: Code 726, NASA Goddard Space Flight Center, Greenbelt, MD 20771.

(1) Rabinovitch, B. S.; Schlag, E. W.; Wiberg, K. B. *J. Chem. Phys.* **1958**, *28*, 504-505.

(2) Setser, D. W.; Rabinovitch, B. S. *J. Am. Chem. Soc.* **1964**, *86*, 564-574.

(3) Baldwin, J. E. *J. Chem. Soc., Chem. Commun.* **1988**, 31-32 and references therein.